Differentially Amplitude- and Phase-Encoded QAM in Amplify-and-Forward Multiple Relay System Over Nakagami-m Fading Channels

Chi-Hua Huang and Char-Dir Chung
Graduate Institute of Communication Engineering
National Taiwan University
Taipei 10617, Taiwan
f95942046@ntu.edu.tw and cdchung@ntu.edu.tw

***Abstract*— This paper studies the differentially amplitude- and phase-encoded (DAPE) quadrature amplitude modulation (QAM) for the amplify-and-forward multiple relay system over independent Nakagami-m fading links. A simple equal gain combining (EGC) receiver is proposed to noncoherently combine received signals from direct and multiple relay links and then detect the DAPE QAM signals without any link side information. Based on Beaulieu's series approach, an efficient bit error probability (BEP) upper bound computation formula is derived for the EGC receiver. Performance results show that the EGC receiver for DAPE QAM provides better BEP than the conventional receiver for differential phase shift keying modulation with the same constellation size.**

***Keywords*—Amplify-and-forward relay, differential detection, Nakagami-m fading, star-QAM.**

I. Introduction

Cooperative relaying technique [1]-[5] is an efficacious method to realize distributed spatial diversity through the cooperation of relay nodes in terms of radio resource and signal processing. In [1]-[2], various cooperative transmission protocols based on half-duplex mode were developed to achieve cooperative diversity. As mentioned therein, the amplify-and-forward (AF) relaying protocol is a simple relaying scheme in which the relays amplify the received signals from the source and retransmit them to the destination. This paper only considers the AF protocol due to its simpler operation and lower complexity required at relays.

Coherent detection is considered in most relay systems, which is based on the assumption that the destination can obtain the channel impulse response (CIR) characteristics of all transmission links [1]-[2]. However, in fast fading environments, it is difficult to obtain the accurate CIR information at the destination through delicate link estimation. To reduce the overhead for complicated link estimation in relay systems, differential modulation has been investigated in [3]-[5]. For the AF multiple relay systems using differential phase shift keying (DPSK) modulation, a weighted gain combining (WGC) receiver was developed in conjunction with approximate bit error probability (BEP) analysis over independent Rayleigh [3] and Nakagami-m [4] fading links. Optimal power allocation for AF multiple relay system based on a simple BEP upper bound was also considered in [3], [5] to improve the overall system performance. Despite a wealth of past studies, the DPSK modulation decreases dramatically in power efficiency when the modulation alphabet size is increased.

The differentially amplitude- and phase-encoded (DAPE) (J_a, J_p) quadrature amplitude modulation (QAM) [6]-[7] is an effective technique to achieve high bit rate transmission without CIR information at the receiver side. DAPE (J_a, J_p) QAM employs a star constellation with J_a concentric amplitude rings, each containing J_p phasors, and sequentially encodes information onto the level changes of amplitude and phase between currently and previously transmitted signals. Due to its higher spectral efficiency and better BEP performance than DPSK, DAPE QAM was extensively studied in [6]-[7] for single link communications. However, DAPE QAM is not yet investigated for relay communications.

This paper studies the DAPE (J_a, J_p) QAM signals for AF multiple relay system over independent Nakagami-m fading links. Section II depicts the system and channel models. In Section III, the conventional EGC receiver in [6]-[7] is adopted to cater to the AF multiple relay system and shown to operate without CIR or any sort of channel state information (CSI) when compared to the noncoherent DPSK WGC and coherent QAM receivers in [1]-[5]. Inevitably, in order to meet the corresponding relay power constraint, the knowledge of average source-relay signal-to-noise power ratio (SNR) is still required at each relay for the EGC receiver, which is a design requirement typical in all differentially coherent AF multiple relay systems [3]-[5]. Based on a union bound argument and a convergent infinite series approach [8], the analytical upper bound of BEP is derived for the EGC receiver over independent Nakagami-m fading links in Section IV. Performance results in Section V show that the EGC receiver for DAPE QAM provides better BEP than the WGC receiver for DPSK with the same constellation size.

Nomenclature: $\mathbb{E}\{\cdot\}$ is the expectation. $\mathcal{Z}_K$ and $\mathcal{Z}_K^+$ denote the integer sets $\{0, 1, ..., K-1\}$ and $\{1, 2, ..., K\}$, respectively. $\mathrm{Re}\{x\}$ is the real part of a complex number x and $\mathrm{Im}\{x\}$ the imaginary part. m mod M denotes the modulo-M value of integer m. Superscript $*$ is the complex conjugate.

 ISBN: 978-1-61208-203-5

II. System and Channel Models

This paper considers the DAPE (J_a, J_p) QAM [6] as the modulation approach. In the DAPE (J_a, J_p) QAM scheme, the transmitted bit sequence corresponding to a nominal N-symbol block is first grouped into $N-1$ independent symbol pairs $\{(\Delta a_n, \Delta b_n)\}_{n=1}^{N-1}$ where $\Delta a_n \in \mathcal{Z}_{J_a}$ and $\Delta b_n \in \mathcal{Z}_{J_p}$. Here, all $J_a J_p$ possible pairs for each $(\Delta a_n, \Delta b_n)$ are assumed to be transmitted equally likely and the binary Gray labeling is used to denote Δa_n and Δb_n individually. The symbols Δa_n and Δb_n are then used to determine the amplitude ratio and the phase difference, respectively, between two consecutively transmitted symbol signals. With $\mu > 1$, the nth transmitted symbol signal is given by $x_n = \lambda \mu^{a_n} e^{j2\pi b_n/J_p}$ for $n \in \mathcal{Z}_{N-1}^+$ and $x_0 = \lambda$ where $\lambda = \sqrt{J_a(\mu^2-1)/(\mu^{2J_a}-1)}$ is used to normalize the signal constellation to unit energy. a_n and b_n represent respectively the amplitude and phase levels of x_n for $n \in \mathcal{Z}_{N-1}^+$ and are given by $a_n = (a_{n-1} + \Delta a_n) \bmod J_a$ and $b_n = (b_{n-1} + \Delta b_n) \bmod J_p$, with $a_0 = b_0 = 0$. Notably, DAPE QAM with $J_a = 1$ corresponds to J_p-ary DPSK.

Consider a multiple relay system which consists of a source node s, a destination node d, and L relay nodes $\{r_l\}_{l=1}^L$. All relays are in a half-duplex mode which can not transmit and receive both in time and frequency simultaneously. In order to avoid mutual interference, it is assumed that the signal transmission scheme includes $L+1$ distinct phases in time. In the first phase, the source broadcasts the signals $\{x_n\}_{n=0}^{N-1}$ with power P_s to all relays and destination. The corresponding nth received symbol signals at destination and relay r_l are

$$y_{sd,n} = \sqrt{P_s \Upsilon_{sd}} h_{sd} x_n + w_{sd,n} \quad (1)$$

$$y_{sl,n} = \sqrt{P_s \Upsilon_{sl}} h_{sl} x_n + w_{sl,n}, \ l \in \mathcal{Z}_L^+ \quad (2)$$

for $n \in \mathcal{Z}_N$. In the $(l+1)$th phase, the relay r_l amplifies its received symbol signals at the first phase to produce $u_{l,n} = \alpha_l y_{sl,n}$ where α_l is the amplification factor and retransmits $\{u_{l,n}\}_{n=0}^{N-1}$ with power P_l to the destination. At the destination, the nth received symbol signal corresponding to the $(l+1)$th phase is

$$y_{ld,n} = \sqrt{P_l \Upsilon_{ld}} h_{ld} u_{l,n} + w_{ld,n}. \quad (3)$$

In the $(L+1)$th phase, the destination then combines all the signals received in all the phases to make a final decision on the information carried by the N-symbol block.

In the above modeling, the coefficients Υ_{ij} and h_{ij} denote respectively the path loss which depends on the geographical distribution of the relay network and the CIR between node i and node j for $ij \in \{sd, \{sl\}_{l=1}^L, \{ld\}_{l=1}^L\}$. Each h_{ij} is assumed constant over an N-symbol block and varies block by block. For analytical convenience, h_{ij}'s are modeled to be independent and have Nakagami-m fading amplitude. For Nakagami-m fading, h_{ij} has independent Nakagami-m distributed amplitude and uniformly distributed phase. The probability density function of a Nakagami-m amplitude $z_{ij} \triangleq |h_{ij}|$ with normalized average power $\mathbb{E}\{|h_{ij}|^2\} = 1$ is $f_{z_{ij}}(z_{ij}) = \frac{2}{\Lambda(m_{ij})} m_{ij}^{m_{ij}} z_{ij}^{2m_{ij}-1} \exp\{-m_{ij} z_{ij}^2\}$ where m_{ij} is the fading parameter, defined by $m_{ij} \triangleq 1/\mathbb{E}\{(z_{ij}^2-1)^2\} \geq 1/2$ [9], and $\Lambda(m) = \int_0^\infty e^{-t} t^{m-1} dt$ is the Gamma function [10]. The additive white Gaussian noise (AWGN) samples $\{w_{ij,n} | ij \in \{sd, \{sl\}_{l=1}^L, \{ld\}_{l=1}^L\}, n \in \mathcal{Z}_N\}$ are modeled as independent and identically distributed (iid) circularly symmetric complex Gaussian random variables (CGRVs) with mean 0 and identical variance σ_w^2. Furthermore, AWGN and fading gains are assumed independent.

In the following, $\gamma_{ij} \triangleq P_i \Upsilon_{ij}/\sigma_w^2$ denotes the average link SNR per symbol from node i to node j for $ij \in \{sd, \{sl\}_{l=1}^L, \{ld\}_{l=1}^L\}$. It is assumed that the total transmission power $P_s + \sum_{l=1}^L P_l = P_t$ is fixed. In the case, $\gamma_t \triangleq P_t/\sigma_w^2$ and $\gamma_b \triangleq \gamma_t/\log_2(J_a J_p)$ are respectively the total transmitted SNRs per symbol and per bit. Moreover, $\hat{\hat{\gamma}}_{sl} \triangleq (1 + \hat{\hat{\delta}}_{sl})\gamma_{sl}$ for $l \in \mathcal{Z}_L^+$ and $\hat{\gamma}_{ij} \triangleq (1 + \hat{\delta}_{ij})\gamma_{ij}$ for $ij \in \{sd, \{sl\}_{l=1}^L, \{ld\}_{l=1}^L\}$ denote respectively the estimate of average link SNR γ_{sl} made at relay r_l and the estimate of average link SNR γ_{ij} made at destination where $\hat{\hat{\delta}}_{sl}$ and $\hat{\delta}_{ij}$ represent the normalized SNR estimation errors. At relay r_l, the amplification factor α_l has to satisfy the respective average relay transmission power constraint $\mathbb{E}\{|\sqrt{P_l}\alpha_l y_{sl,n}|^2\} = P_l$ and is given by $\alpha_l = 1/(\sigma_w \sqrt{\gamma_{sl}+1})$ for $l \in \mathcal{Z}_L^+$ [3]-[5]. Notably, the average link SNR γ_{sl} is required for realizing α_l and can be measured through conventional SNR estimation methods [11]. With SNR estimation, γ_{sl} in α_l can be replaced by an estimate $\hat{\hat{\gamma}}_{sl}$ for capturing the impact of SNR estimation error. Since the noise variance σ_w^2 remains constant over long periods of time in practice, it is assumed to be perfectly measured.

III. Decision Algorithm

In this section, a symbol-by-symbol decision algorithm for detecting $(\Delta a_n, \Delta b_n)$ is derived based on the received symbol signals $\{y_{sd,n-1}, y_{sd,n}\}$ and $\{y_{ld,n-1}, y_{ld,n}\}_{l=1}^L$ for $n \in \mathcal{Z}_{N-1}^+$. For notational brevity, the subscript n in $(\Delta a_n, \Delta b_n)$ is dropped below.

The EGC receiver [6]-[7] is commonly used for demodulating DAPE (J_a, J_p) QAM with multiple received antennas and can be applied here for the AF multiple relay system. Specifically, the EGC receiver makes amplitude and phase decisions separately. The amplitude decision is based on detecting the amplitude ratio of successively received symbol signals in $\{y_{sd,n-1}, y_{sd,n}\}$ and $\{y_{ld,n-1}, y_{ld,n}\}_{l=1}^L$ in conjunction with square-law combining. The test metric on amplitude ratio is given by

$$W_a = \frac{|y_{sd,n}|^2 + \sum_{l=1}^L q_l |y_{ld,n}|^2}{|y_{sd,n-1}|^2 + \sum_{l=1}^L q_l |y_{ld,n-1}|^2} \quad (4)$$

where $q_l \triangleq 1$ for $l \in \mathcal{Z}_L^+$. Thus, the amplitude decision rule is to declare $\Delta\hat{a} = k$ if $W_a \in R_k$, where the amplitude decision region R_k is defined by $R_k \triangleq \{W_a | \eta_k^2 \leq W_a < \eta_{k+1}^2$ or $\eta_{k-J_a}^2 \leq W_a < \eta_{k-J_a+1}^2\}$ for $k \in \mathcal{Z}_{J_a-1}^+$ and $R_0 \triangleq \{W_a | \eta_0^2 \leq W_a < \eta_1^2\}$ with $0 = \eta_{-J_a+1} < \eta_{-J_a+2} < \ldots < \eta_{J_a} = \infty$. The amplitude decision threshold η_k is given by

$\eta_k = \mu^{k-1/2}$ for $k = -J_a+2, -J_a+3, ..., J_a-1$ as in [6].[1] On the other hand, the differential phase decision is based on the conventional product detector for demodulating J_p-ary DPSK with multiple observations [9], and the test metric on phase difference is given by

$$W_p = y_{sd,n}y_{sd,n-1}^* + \sum_{l=1}^{L} q_l y_{ld,n}y_{ld,n-1}^*. \tag{5}$$

Thus, the phase decision rule is to declare $\Delta\widehat{b}$ if $\mathrm{Re}\{W_p e^{-j2\pi\Delta b/J_p}\}$ is maximized when $\Delta b = \Delta\widehat{b}$.

Notably, for the WGC receiver detecting J_p-ary DPSK in [3]-[5], the test metric on phase difference is the same as (5) with $q_l = 1$ replaced by $q_l = (1+\widehat{\gamma}_{sl})/(1+\widehat{\gamma}_{sl}+\widehat{\gamma}_{ld})$ for $l \in \mathcal{Z}_L^+$, where the link SNR estimates $\widehat{\gamma}_{sl}$ and $\widehat{\gamma}_{ld}$ can be measured prior to data detection at destination through SNR estimation methods [11].[2] Therefore, the phase decision rule of the WGC receiver for J_p-ary DPSK is to declare $\Delta\widehat{b}$ if $\mathrm{Re}\{W_p e^{-j2\pi\Delta b/J_p}\}$ is maximized when $\Delta b = \Delta\widehat{b}$.

IV. BEP ANALYSIS

In this section, the BEP upper bound of EGC receiver is analyzed below for independent Nakagami-m fading links.

A) BEP Characteristics: The average BEP can be generally expressed as [6]-[7]

$$\mathcal{P}_b = \frac{\mathcal{P}_a \log_2 J_a + \mathcal{P}_p \log_2 J_p}{\log_2(J_a J_p)} \tag{6}$$

where $\mathcal{P}_a$ and $\mathcal{P}_p$ are the average BEPs for detecting amplitude ratio and phase difference, respectively. Specifically, $\mathcal{P}_a$ and the union bound for $\mathcal{P}_p$ are given by

$$\mathcal{P}_a = \frac{1}{J_a}\sum_{\substack{\Delta a, \Delta\widehat{a}=0 \\ \Delta a \neq \Delta\widehat{a}}}^{J_a-1} \frac{c(\Delta a, \Delta\widehat{a})}{\log_2 J_a}\mathcal{P}_1(\Delta\widehat{a}|\Delta a) \tag{7}$$

$$\mathcal{P}_p \leq \frac{1}{J_p}\sum_{\substack{\Delta b, \Delta\widehat{b}=0 \\ \Delta b \neq \Delta\widehat{b}}}^{J_p-1} \frac{c(\Delta b, \Delta\widehat{b})}{\log_2 J_p} \cdot\frac{1}{J_a^2}\sum_{a_{n-1}=0}^{J_a-1}\sum_{a_n=0}^{J_a-1}\mathcal{P}_2(\Delta\widehat{b}|a_{n-1}, a_n, \Delta b). \tag{8}$$

Here, $c(i,j)$ is the Hamming distance between the binary representations of i and j. $\mathcal{P}_1(\Delta\widehat{a}|\Delta a)$ represents the probability of deciding $\Delta\widehat{a}$ (i.e., $W_a \in R_{\Delta\widehat{a}}$) given that Δa is transmitted. $\mathcal{P}_2(\Delta\widehat{b}|a_{n-1}, a_n, \Delta b) \triangleq \Pr\{\mathrm{Re}\{W_p e^{-j2\pi\Delta b/J_p}\} < \mathrm{Re}\{W_p e^{-j2\pi\Delta\widehat{b}/J_p}\}|a_{n-1}, a_n, \Delta b\}$ denotes the pairwise error probability that $\mathrm{Re}\{W_p e^{-j2\pi\Delta\widehat{b}/J_p}\}$ is larger than $\mathrm{Re}\{W_p e^{-j2\pi\Delta b/J_p}\}$ given that a_{n-1}, a_n, and Δb are transmitted. Using (7) and (8) in (6) gives an upper bound to the BEP of the EGC receiver.[3]

The evaluation of $\mathcal{P}_1(\Delta\widehat{a}|\Delta a)$ has to be separately treated for two cases $\Delta\widehat{a} = 0$ and $\Delta\widehat{a} \neq 0$ since different decision region formats are involved. $\mathcal{P}_1(\Delta\widehat{a}|\Delta a)$ is given by[4]

$$\mathcal{P}_1(0|\Delta a) = \frac{1}{J_a}\sum_{a_{n-1}=0}^{J_a-1-\Delta a}\mathcal{P}_3(0|a_{n-1}, a_{n-1}+\Delta a) + \frac{1}{J_a}\sum_{a_{n-1}=J_a-\Delta a}^{J_a-1}\mathcal{P}_3(0|a_{n-1}, a_{n-1}+\Delta a - J_a) \tag{9}$$

when $\Delta\widehat{a} = 0$, and

$$\begin{aligned}\mathcal{P}_1(\Delta\widehat{a}|\Delta a) = {} & \frac{1}{J_a}\sum_{a_{n-1}=0}^{J_a-1-\Delta a}[\mathcal{P}_3(\Delta\widehat{a}|a_{n-1}, a_{n-1}+\Delta a) \\ & +\mathcal{P}_3(\Delta\widehat{a}-J_a|a_{n-1}, a_{n-1}+\Delta a)] \\ & +\frac{1}{J_a}\sum_{a_{n-1}=J_a-\Delta a}^{J_a-1}[\mathcal{P}_3(\Delta\widehat{a}|a_{n-1}, a_{n-1}+\Delta a - J_a) \\ & +\mathcal{P}_3(\Delta\widehat{a}-J_a|a_{n-1}, a_{n-1}+\Delta a - J_a)]\end{aligned} \tag{10}$$

when $\Delta\widehat{a} \in \mathcal{Z}_{J_a-1}^+$. In (9) and (10), $\mathcal{P}_3(k|a_{n-1}, a_n) \triangleq \Pr\{\eta_k^2 \leq W_a < \eta_{k+1}^2|a_{n-1}, a_n\}$ denotes the conditional probability of event $\{\eta_k^2 \leq W_a < \eta_{k+1}^2\}$ given that a_{n-1} and a_n are transmitted. Note here that $\Pr\{\eta_k^2 \leq W_a < \eta_{k+1}^2|a_{n-1}, a_n\}$ can be alternatively expressed and thus evaluated as $\Pr\{W_a < \eta_{k+1}^2|a_{n-1}, a_n\} - \Pr\{W_a < \eta_k^2|a_{n-1}, a_n\}$.

Both events $\{W_a < \eta_k^2\}$ and $\{\mathrm{Re}\{W_p e^{-j2\pi\Delta b/J_p}\} < \mathrm{Re}\{W_p e^{-j2\pi\Delta\widehat{b}/J_p}\}\}$ in evaluating respectively $\Pr\{W_a < \eta_k^2|a_{n-1}, a_n\}$, which is required for computing $\mathcal{P}_1(\Delta\widehat{a}|\Delta a)$ in (7), and $\mathcal{P}_2(\Delta\widehat{b}|a_{n-1}, a_n, \Delta b)$ in (8) can be conveniently unified in the form of $\{X_i + \sum_{l=1}^{L} Y_{l,i} < 0\}$, in which the variables X_i and $Y_{l,i}$ are defined as $X_i \triangleq A_i\left|y_{sd,n}/\sigma_w\right|^2 + B_i\left|y_{sd,n-1}/\sigma_w\right|^2 + 2\,\mathrm{Re}\{C_i y_{sd,n}y_{sd,n-1}^*/\sigma_w^2\}$ and $Y_{l,i} \triangleq D_{l,i}\left|y_{ld,n}/\sigma_w\right|^2 + E_{l,i}\left|y_{ld,n-1}/\sigma_w\right|^2 + 2\,\mathrm{Re}\{F_{l,i}y_{ld,n}y_{ld,n-1}^*/\sigma_w^2\}$, respectively, for $l \in \mathcal{Z}_L^+$ and $i \in \{a, p\}$.[5] The coefficient vector $(A_i, B_i, C_i, D_{l,i}, E_{l,i}, F_{l,i})$ is set to $(1, -\eta_k^2, 0, q_l, -q_l\eta_k^2, 0)$ for event $\{W_a < \eta_k^2\}$ (when $i = a$) and $(0, 0, e^{-j2\pi\Delta b/J_p} - e^{-j2\pi\Delta\widehat{b}/J_p}, 0, 0, q_l(e^{-j2\pi\Delta b/J_p} - e^{-j2\pi\Delta\widehat{b}/J_p}))$ for event $\{\mathrm{Re}\{W_p e^{-j2\pi\Delta b/J_p}\} < \mathrm{Re}\{W_p e^{-j2\pi\Delta\widehat{b}/J_p}\}\}$ (when $i = p$). In terms of the unified format, $\Pr\{W_a < \eta_k^2|a_{n-1}, a_n\}$ and $\mathcal{P}_2(\Delta\widehat{b}|a_{n-1}, a_n, \Delta b)$ can be both expressed as $\Pr\{X_i + \sum_{l=1}^{L} Y_{l,i} < 0|\mathcal{S}\}$ given $\mathcal{S} \triangleq \{a_{n-1}, a_n, \Delta b\}$.

[1]Due to cyclic differential amplitude encoding, when $\Delta a \neq 0$ the two possible cases $|x_n|/|x_{n-1}| > 1$ and $|x_n|/|x_{n-1}| < 1$ must be considered in amplitude decision. This explains that R_k for $k \neq 0$ consists of two disjoint regions where $\{W_a|\eta_k^2 \leq W_a < \eta_{k+1}^2\}$ accounts for the case $|x_n| > |x_{n-1}|$ and $\{W_a|\eta_{k-J_a}^2 \leq W_a < \eta_{k-J_a+1}^2\}$ for the case $|x_n| < |x_{n-1}|$.

[2]As indicated, the EGC receiver for DAPE QAM operates without any CSI, while the knowledge of average SNR estimates on source-relay and relay-destination links is required for realizing the WGC receiver for DPSK.

[3]As mentioned previously, the test metric on phase difference W_p is of the same form for both EGC and WGC receivers except for gain variables $\{q_l\}_{l=1}^{L}$. Thus, when $J_a = 1$, (6) also gives an upper bound to the BEP of the WGC receiver for J_p-ary DPSK [3]-[5].

[4]By default, $\sum_{k=n}^{m} = 0$, if $n > m$.

[5]Here, the subscript i used for the variables X_i and $Y_{l,i}$ denotes the respective cases for event $\{W_a < \eta_k^2\}$ (when $i = a$) and event $\{\mathrm{Re}\{W_p e^{-j2\pi\Delta b/J_p}\} < \mathrm{Re}\{W_p e^{-j2\pi\Delta\widehat{b}/J_p}\}\}$ (when $i = p$).

 ISBN: 978-1-61208-203-5

Based on Beaulieu's convergent infinite series approach proposed by [8], $\Pr\{X_i + \sum_{l=1}^{L} Y_{l,i} < 0|\mathcal{S}\}$ can be efficiently evaluated within a predetermined accuracy as

$$\Pr\left\{X_i + \sum_{l=1}^{L} Y_{l,i} < 0|\mathcal{S}\right\} \approx \frac{1}{2} - \frac{2}{\pi} \sum_{\substack{m=1 \\ m\ odd}}^{\infty} \frac{1}{m} \cdot \mathrm{Im}\left\{\Phi_{X_i}(jm\omega_0|\mathcal{S}) \prod_{l=1}^{L} \Phi_{Y_{l,i}}(jm\omega_0|\mathcal{S})\right\} \quad (11)$$

where $j \triangleq \sqrt{-1}$, $\omega_0 \triangleq 2\pi/T$ with T being the period of the square wave used in deriving the series, and $\Phi_{X_i}(j\omega|\mathcal{S})$ and $\Phi_{Y_{l,i}}(j\omega|\mathcal{S})$ represent respectively the conditional characteristic functions (CFs) of X_i and $Y_{l,i}$ given $\mathcal{S}$. The series in (11) converges pointwise to the true distribution value within a specific accuracy when T is chosen large enough and can be thus truncated to a desired accuracy. To facilitate the evaluation of (11), analytical expressions for $\Phi_{X_i}(j\omega|\mathcal{S})$ and $\Phi_{Y_{l,i}}(j\omega|\mathcal{S})$ are derived in the following.

B) Characteristic Functions $\Phi_{X_i}(j\omega|\mathcal{S})$ and $\Phi_{Y_{l,i}}(j\omega|\mathcal{S})$: Conditioned on $\mathcal{S}$ and h_{sd}, $y_{sd,n}$ and $y_{sd,n-1}$ are jointly CGRVs, and thus X_i is a conditionally Gaussian quadratic sum (GQS) [9]. Quoting [9, eq. (B-5)], $\Phi_{X_i}(j\omega|\mathcal{S}, h_{sd})$ is readily given by

$$\Phi_{X_i}(j\omega|\mathcal{S}, z_{sd}) = \frac{1}{H_i(\omega)} \exp\left\{\frac{G_i(\omega) z_{sd}^2}{H_i(\omega)}\right\} \quad (12)$$

where $G_i(\omega) \triangleq \gamma_{sd}\{\omega^2(A_iB_i - |C_i|^2)(|x_n|^2 + |x_{n-1}|^2) + j\omega[A_i|x_n|^2 + B_i|x_{n-1}|^2 + 2\,\mathrm{Re}\{C_i x_n x_{n-1}^*\}]\}$ and $H_i(\omega) \triangleq 1 - j\omega(A_i + B_i) + \omega^2(|C_i|^2 - A_iB_i)$. Similarly, conditioned on $\mathcal{S}$, h_{sl}, and h_{ld}, $y_{ld,n}$ and $y_{ld,n-1}$ are jointly CGRVs, and thus $Y_{l,i}$ is also a conditionally GQS. $\Phi_{Y_{l,i}}(j\omega|\mathcal{S}, z_{sl}, z_{ld})$ can also be derived from [9, eq. (B-5)] as

$$\Phi_{Y_{l,i}}(j\omega|\mathcal{S}, z_{sl}, z_{ld}) = \frac{1}{V_{l,i}(\omega|z_{ld})} \exp\left\{\frac{U_{l,i}(\omega|z_{ld}) z_{sl}^2}{V_{l,i}(\omega|z_{ld})}\right\} \quad (13)$$

where $U_{l,i}(\omega|z_{ld}) \triangleq \gamma_{sl}\upsilon\{\omega^2\kappa(1+\upsilon)(|x_n|^2 + |x_{n-1}|^2) + j\omega[D_{l,i}|x_n|^2 + E_{l,i}|x_{n-1}|^2 + 2\,\mathrm{Re}\{F_{l,i}x_n x_{n-1}^*\}]\}$ and $V_{l,i}(\omega|z_{ld}) \triangleq 1 - (1+\upsilon)^2[j\omega(D_{l,i} + E_{l,i})/(1+\upsilon) + \omega^2\kappa]$ with $\upsilon \triangleq \gamma_{ld} z_{ld}^2 \alpha_l^2 \sigma_w^2$ and $\kappa \triangleq D_{l,i}E_{l,i} - |F_{l,i}|^2$. Thus, $\Phi_{X_i}(j\omega|\mathcal{S})$ and $\Phi_{Y_{l,i}}(j\omega|\mathcal{S})$ can be respectively obtained by averaging $\Phi_{X_i}(j\omega|\mathcal{S}, z_{sd})$ over the density of z_{sd} and $\Phi_{Y_{l,i}}(j\omega|\mathcal{S}, z_{sl}, z_{ld})$ over the joint density of z_{sl} and z_{ld}, as given below.

1) Characteristic Function $\Phi_{X_i}(j\omega|\mathcal{S})$: Using [12, eq. (3.478.1)], averaging $\Phi_{X_i}(j\omega|\mathcal{S}, z_{sd})$ over $f_{z_{sd}}(z_{sd})$ gives the CF $\Phi_{X_i}(j\omega|\mathcal{S})$ as

$$\Phi_{X_i}(j\omega|\mathcal{S}) = \frac{1}{H_i(j\omega)} \left[\frac{H_i(j\omega)}{H_i(j\omega) - G_i(j\omega)/m_{sd}}\right]^{m_{sd}}. \quad (14)$$

2) Characteristic Function $\Phi_{Y_{l,i}}(j\omega|\mathcal{S})$: Note that $\Phi_{Y_{l,i}}(j\omega|\mathcal{S}, z_{sl}, z_{ld})$ in (13) is exactly of the same expression as $\Phi_{X_i}(j\omega|\mathcal{S}, z_{sd})$ in (12) with z_{sd}, $G_i(\omega)$, and $H_i(\omega)$ respectively replaced by z_{sl}, $U_{l,i}(\omega|z_{ld})$, and $V_{l,i}(\omega|z_{ld})$. Thus, by virtue of the independence between z_{sl} and z_{ld}, $\Phi_{Y_{l,i}}(j\omega|\mathcal{S}, z_{ld})$ can be similarly obtained as the expressions in (14) with $G_i(\omega) \to U_{l,i}(\omega|z_{ld})$, $H_i(\omega) \to V_{l,i}(\omega|z_{ld})$, and $m_{sd} \to m_{sl}$ after averaging $\Phi_{Y_{l,i}}(j\omega|\mathcal{S}, z_{sl}, z_{ld})$ over $f_{z_{sl}}(z_{sl})$. By averaging the resultant $\Phi_{Y_{l,i}}(j\omega|\mathcal{S}, z_{ld})$ over $f_{z_{ld}}(z_{ld})$, the CF $\Phi_{Y_{l,i}}(j\omega|\mathcal{S})$ can be obtained as

$$\Phi_{Y_{l,i}}(j\omega|\mathcal{S}) = \int_0^{\infty} \Phi_{Y_{l,i}}(j\omega|\mathcal{S}, z_{ld}) f_{z_{ld}}(z_{ld}) dz_{ld}. \quad (15)$$

Unfortunately, the single integral in (15) is difficult, if not impossible, to complete. However, it can be numerically computed by Gaussian quadrature rule [10, eq. (25.4.45)].

V. PERFORMANCE RESULTS

This section illustrates the BEP results of the EGC receiver in conjunction with DAPE (J_a, J_p) QAM formats with constellation sizes $J_aJ_p = 64$ over iid Nakagami-m fading links. For notational brevity, the subscript ij in Nakagami-m fading parameter m_{ij} is dropped. The BEP characteristics for the EGC receiver is evaluated by using the BEP upper bound expressions (6)-(8) as well as Monte Carlo simulation. For simplicity, it is also assumed that all source-relay path losses, all relay-destination path losses, and all transmission powers are respectively identical with $\Upsilon_{sl} = \Upsilon_{sr}$, $\Upsilon_{ld} = \Upsilon_{rd}$, and $P_l = P_s = P_t/(L+1)$ for all $l \in \mathcal{Z}_L^+$. In the presence of SNR estimation errors, it is further assumed that all source-relay links suffer the same level of error and so do relay-destination links, with $\widehat{\widehat{\delta}}_{sl} = \widehat{\widehat{\delta}}_{sr}$, $\widehat{\delta}_{sl} = \widehat{\delta}_{sr}$, and $\widehat{\delta}_{ld} = \widehat{\delta}_{rd}$ for all $l \in \mathcal{Z}_L^+$. Moreover, the estimate $\widehat{\widehat{\gamma}}_{sl}$ made at relay r_l is assumed to be delivered to the destination through a very reliable transmission link, and thus $\widehat{\widehat{\gamma}}_{sl}$ is equal to the estimate $\widehat{\gamma}_{sl}$ made at destination for all $l \in \mathcal{Z}_L^+$ (i.e., $\widehat{\widehat{\delta}}_{sr} = \widehat{\delta}_{sr}$).

The BEP of a DAPE QAM system with a fixed constellation size depends on the setting of ring ratio μ and (J_a, J_p) [6]-[7]. By minimizing the BEP upper bound expressions, the optimization of μ and (J_a, J_p) can be achieved. As observed by the authors, when μ is optimized, DAPE $(4, 16)$ QAM gives the best BEP performance in all possible 64-point constellations for wide ranges of m and γ_b. Moreover, the BEP upper bound achieves nearly the best when μ is fixed to 1.4 for DAPE $(4, 16)$ QAM, and thus this value for μ is adopted below.

Figs. 1-2 compare the BEP characteristics among the EGC receiver for DAPE $(4, 16)$ QAM and 64-ary DPSK and the WGC receiver for 64-ary DPSK [3]-[5]. Fig. 1 illustrates the BEP characteristics for various scenarios with different geographical relay locations. The scenarios represent that all relays are close to the source when Υ_{sr} is larger than Υ_{rd} and that all relays are close to the destination when Υ_{rd} is larger than Υ_{sr} [3]. As indicated, the EGC receiver under the scenario $\Upsilon_{sr} > \Upsilon_{rd}$ performs better than that under the scenario $\Upsilon_{rd} > \Upsilon_{sr}$, but this performance prevalence is reversed for the WGC receiver. The difference in the performance trends between the EGC and WGC receivers comes from the settings of the gain variables $\{q_l\}_{l=1}^{L}$ that the average source-relay and relay-destination link SNRs are not leveraged by the

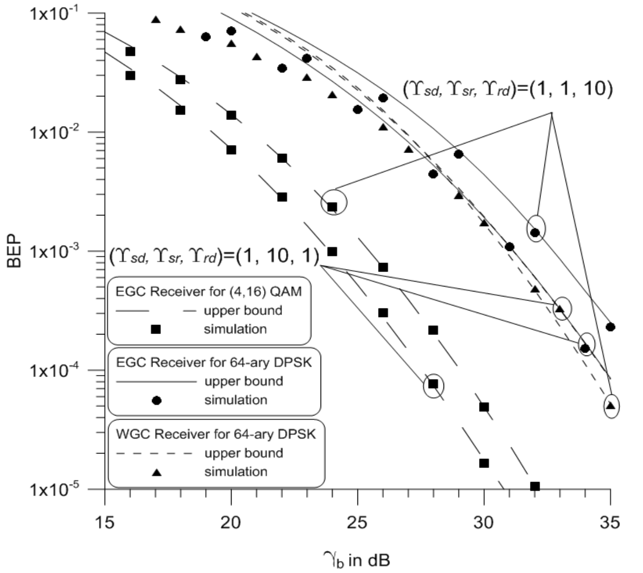

Fig. 1. BEP versus SNR/bit characteristics of EGC receiver for DAPE $(4, 16)$ QAM and 64-ary DPSK and WGC receiver for 64-ary DPSK with $\widehat{\delta}_{sr} = \widehat{\delta}_{rd} = 0$, $m = 1.5$, and $L = 2$.

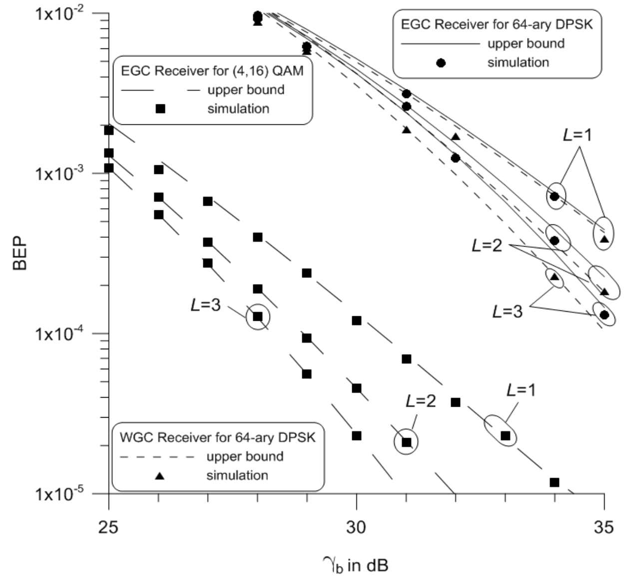

Fig. 2. BEP versus SNR/bit characteristics of EGC receiver for DAPE $(4, 16)$ QAM and 64-ary DPSK and WGC receiver for 64-ary DPSK with $\widehat{\delta}_{sr} = \widehat{\delta}_{rd} = 0$, $m = 1.5$, and $(\Upsilon_{sd}, \Upsilon_{sr}, \Upsilon_{rd}) = (1, 1, 1)$.

EGC receiver but used by the WGC receiver. Thus, the EGC receiver suffers the BEP performance degradation under the scenario $\Upsilon_{rd} > \Upsilon_{sr}$. As also observed, when $\Upsilon_{sr} \gg \Upsilon_{rd}$ (e.g., $(\rho_{sr}, \rho_{rd}) = (10, 1)$), the EGC and WGC receivers for DPSK perform almost the same because the gain variable of the WGC receiver $q_l \approx 1$ for all $l \in \mathcal{Z}_L$, and both EGC and WGC receivers for DPSK are approximately equivalent. Fig. 2 shows that the diversity reception can effectively improve the BEP performance. This performance improvement is, however, achieved at the cost of using more relays as well as reducing overall network throughput [4]. As indicated in Figs. 1-2, the EGC receiver for DAPE QAM significantly outperforms the EGC and WGC receivers for DPSK. As also observed, the BEP upper bounds for both EGC and WGC receivers are in the better agreement with simulation when the average link SNRs are sufficiently larger and $L > 1$.

Fig. 3 demonstrates the BEP characteristics of EGC receiver for DAPE QAM and DPSK as well as WGC receiver for DPSK with link SNR estimation errors. Because the test metrics depend on link SNR estimates for the WGC receiver but not for the EGC receiver, in addition to the requirement that all relay gains depend on source-relay link SNR estimates, the EGC receiver for DAPE QAM degrades in BEP less than the WGC receiver in the presence of link SNR estimation errors. This explains that the EGC receiver is less sensitive to link SNR estimation errors than the WGC receiver.

Fig. 4 compares the BEP characteristics among the EGC receiver for DAPE $(4, 16)$ QAM, the WGC receiver for 64-ary DPSK, and maximum-likelihood (ML) receiver [2] for coherent 64-ary rectangular QAM with Gray labeling. For the coherent ML receiver, the decision rule is to declare the

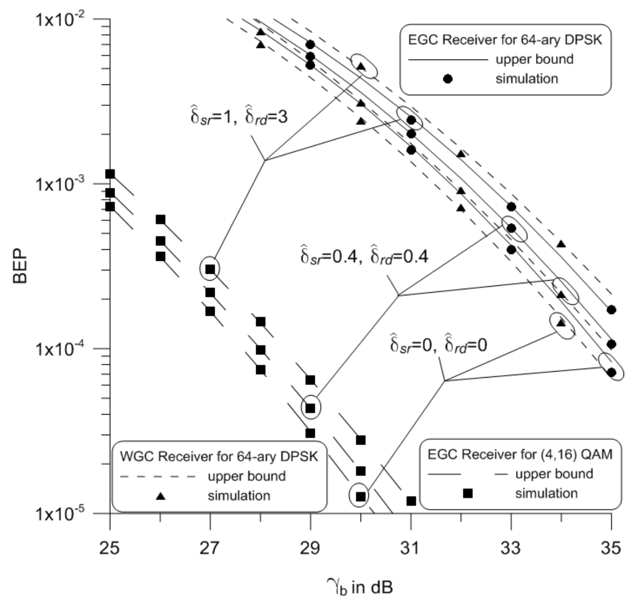

Fig. 3. BEP versus SNR/bit characteristics of EGC receiver for DAPE $(4, 16)$ QAM and 64-ary DPSK and WGC receiver for 64-ary DPSK with $m = 2$, $L = 2$, and $(\Upsilon_{sd}, \Upsilon_{sr}, \Upsilon_{rd}) = (1, 1, 1)$.

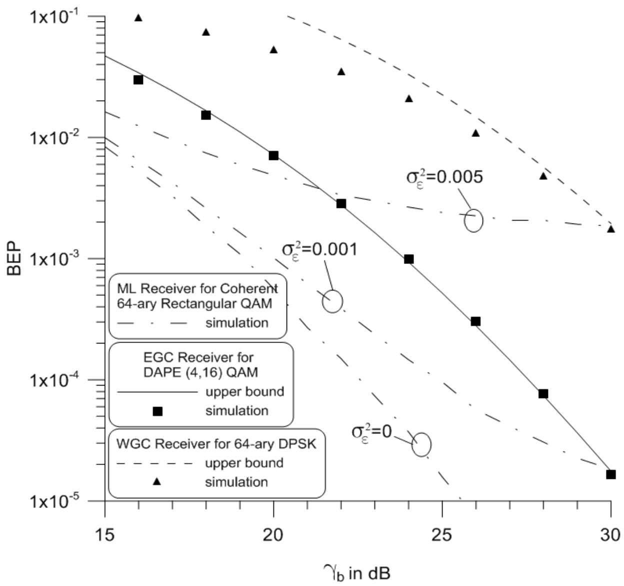

Fig. 4. BEP versus SNR/bit characteristics of EGC receiver for DAPE $(4, 16)$ QAM, WGC receiver for 64-ary DPSK, and ML receiver for coherent 64-ary rectangular QAM with $\widehat{\delta}_{sd} = \widehat{\delta}_{sr} = \widehat{\delta}_{rd} = 0$, $m = 1.5$, $L = 2$, and $(\Upsilon_{sd}, \Upsilon_{sr}, \Upsilon_{rd}) = (1, 10, 1)$.

decision $\widehat{x}_n$ corresponding to

$$\max_{x_n \in \varkappa} \mathrm{Re}\{\vartheta x_n^*\} - \frac{|x_n|^2}{2} \left[\widehat{\gamma}_{sd} \widehat{z}_{sd}^2 + \sum_{l=1}^{L} \frac{\sigma_w^2 \alpha_l^2 \widehat{\gamma}_{sl} \widehat{\gamma}_{ld} \widehat{z}_{sl}^2 \widehat{z}_{ld}^2}{1 + \sigma_w^2 \alpha_l^2 \widehat{\gamma}_{ld} \widehat{z}_{ld}^2} \right] \tag{16}$$

where the parameter ϑ is defined as

$$\vartheta \triangleq \frac{\sqrt{\widehat{\gamma}_{sd}} \widehat{h}_{sd}^* y_{sd,n}}{\sigma_w} + \sum_{l=1}^{L} \frac{\alpha_l \sqrt{\widehat{\gamma}_{sl} \widehat{\gamma}_{ld}} \widehat{h}_{sl}^* \widehat{h}_{ld}^* y_{ld,n}}{1 + \sigma_w^2 \alpha_l^2 \widehat{\gamma}_{ld} \widehat{z}_{ld}^2}$$

and $\varkappa \triangleq \{\pm\beta, \pm 3\beta, ..., \pm(I-1)\beta\}$ with $\beta = \sqrt{3/(2I^2-2)}$ denotes the I^2-ary rectangular QAM symbol set. Notably, the knowledge of the average SNR estimates $\widehat{\gamma}_{ij}$'s and the CIR estimates $\widehat{h}_{ij}$'s made at destination and the amplification factors α_l's used at relays are all required for realizing the coherent ML receiver. In addition to link SNR estimates, the requirement of link CIR estimates at destination complicates to a great extent the design of the coherent ML receiver when compared to both noncoherent EGC and WGC receivers.

With perfect link SNR estimation (i.e., $\widehat{\delta}_{sd} = \widehat{\delta}_{sl} = \widehat{\delta}_{ld} = 0$ for $l \in \mathcal{Z}_L^+$), the effect of incorrect CIR estimation is also shown in Fig. 4 to illustrate the sensitivity of the coherent receiver to CIR information. Specifically, we denote $\widehat{h}_{ij} \triangleq h_{ij} + \varepsilon_{ij}$ for $ij \in \left\{sd, \{sl\}_{l=1}^L, \{ld\}_{l=1}^L\right\}$ where the estimation error ε_{ij} is modeled as a CGRV with mean 0 and variance $\sigma_{\varepsilon,ij}^2$ [11] which is mutually independent and independent of the CIRs h_{ij}'s. For presentation simplicity, it is further assumed that all the CIR estimation errors have the same variance, i.e., $\sigma_{\varepsilon,ij} = \sigma_\varepsilon$. As shown in Fig. 4, the coherent ML receiver significantly outperforms noncoherent EGC and WGC receivers when the CIR estimation is correct. In the presence of CIR estimation errors, the coherent ML receiver degrades more significantly with larger errors and exhibits severe error-rate floors in high SNR region, where both noncoherent EGC and WGC receivers prevail.

VI. Conclusion

In this paper, the EGC receiver is developed to noncoherently combine received signals from direct and relay links and then demodulate DAPE QAM signals in the AF multiple relay system over independent Nakagami-m fading links. The EGC receiver for DAPE QAM is simpler to implement than noncoherent DPSK WGC and coherent QAM receivers since it is devoid of any CSI. Based on Beaulieu's series approach, an efficient BEP upper bound computation formula is analytically derived for the EGC receiver. The BEP upper bound is verified by simulation to be tight when the average link SNRs are sufficiently large. Performance results show that the EGC receiver for DAPE QAM performs much better than the WGC receiver for DPSK with the same constellation size. Moreover, the EGC receiver is shown to be less sensitive to SNR estimation errors than the WGC receiver for DPSK.

VII. Ackownledgement

This work was supported in part by the National Science Council of Taiwan under Contract NSC-100-2221-E-002-125-MY2 and by the National Taiwan University through the Excellent Research Project under Grant 10R80919-4.

References

[1] J. N. Laneman, D. N. C. Tse, and G. W. Wornell, "Cooperative diversity in wireless networks: Efficient protocols and outage behavior," *IEEE Trans. Inform. Theory*, vol. 50, no. 12, pp. 3062–3080, Dec. 2004.
[2] J. N. Laneman and G. W. Wornell, "Energy-efficient antenna sharing and relaying for wireless networks," in *Proc. IEEE Wireless Commun. and Networking Conf.*, Chicago, IL, Sep. 23-28, 2000, vol. 1, pp. 7-12.
[3] T. Himsoon, W. P. Siriwongpairat, W. Su, and K. J. R. Liu, "Differential modulations for multinode cooperative communications," *IEEE Trans. Signal Process.*, vol. 56, no. 7, pp. 2941–2956, Jul. 2008.
[4] S. S. Ikki and M. H. Ahmed, "Performance of cooperative diversity using equal gain combining (EGC) over Nakagami-m fading channels," *IEEE Trans. Wireless Commun.*, vol. 8, no. 2, pp. 557–562, Feb. 2009.
[5] W. Cho, R. Cao, and L. Yang, "Optimum resource allocation for amplify-and-forward relay networks with differential modulation," *IEEE Trans. Signal Process.*, vol. 56, no. 11, pp. 5680–5691, Nov. 2008.
[6] C.-D. Chung, "Differentially amplitude and phase-encoded QAM for the correlated Rayleigh-fading channel with diversity reception," *IEEE Trans. Commun.*, vol. 45, no. 3, pp. 309–321, Mar. 1997.
[7] Y. Ma, Q. T. Zhang, R. Schober, and S. Pasupathy, "Diversity reception of DAPSK over generalized fading channels," *IEEE Trans. Wireless Commun.*, vol. 4, no. 4, pp. 1834-1846, Jul. 2005.
[8] N. C. Beaulieu, "An infinite series for the computation of the complementary probability distribution function of a sum of independent random variables and its application to the sum of Rayleigh random variables," *IEEE Trans. Commun.*, vol. 38, no. 9, pp. 1463–1474, Sep. 1990.
[9] J. G. Proakis, *Digital Communications*, 4th ed. New York: McGraw-Hill, 2001.
[10] M. Abramowitz and I. A. Stegun, *Handbook of Mathematical Functions With Formulas, Graphs, and Mathematical Tables*, 9th ed. New York: Dover, 1970.
[11] S. Roy and P. Fortier, "Maximal-ratio combining architectures and performance with channel estimation based on a training sequence," *IEEE Trans. Wireless Commun.*, vol. 3, no. 4, pp. 1154-1164, Jul. 2004.
[12] I. S. Gradshteyn and I. M. Ryzhik, *Table of Integrals, Series, and Products*, 6th ed. San Diego, CA: Academic Press, 2000.